Electronic Supplementary Information

Sensitive Photoelectrochemical Assay of Pb^{2+} Based on DNAzyme-Induced Disassembly of "Z-Scheme" TiO_2/Au/CdS QDs System

Leixia Meng, Mengyue Liu, Ke Xiao, Xiaohua Zhang, Cuicui Du, Jinhua Chen*

State Key Laboratory of Chemo/Biosensing and Chemometrics, College of Chemistry and Chemical Engineering, Hunan University, Changsha, 410082, People's Republic of China

List of Contents:

* Corresponding author. Tel.: +86-731-88821848

E-mail address: chenjinhua@hnu.edu.cn

1. Materials and apparatus

TiO_2 powder (P25) was purchased from the Degussa Co. (Germany). Cadmium chloride hemipentahydrate ($CdCl_2 \cdot 2.5H_2O$), sodiumborohydride (NaBH4), thioacetamide (TAA), tris-(hydroxymethyl) aminomethane (Tris), ethylenediaminetetraacetic acid (EDTA) and ascorbic acid (AA) were purchased from Sinopharm Chemical Reagent Co., Ltd. (Beijing, China). Carbodiimide hydrochloride (EDC), N-hydroxysuccinimide (NHS) and 6-mercaptohexanol (MCH) were purchased from Sigma-Aldrich Co., Ltd. (USA). Mercaptopropionic acid (MPA, 98%) and hydrogen tetrachloroaurate (III) trihydrate (HAuCl4·3H2O, 99.999%) were obtained from Macklin Reagent Co., Ltd. (Shanghai, China). Tris (2-carboxyethyl) phosphinehydrochloride (TCEP) were ordered from Sangon Biotechnology Co., Ltd. (Shanghai, China). The normal human serum was supplied by Anyan Trade Co., Ltd (Shanghai, China). The indium tin oxide (ITO) glass was purchased from Zhuhai Kaivo Electronic Components Co., Ltd. (China). All the synthetic DNA strands were supplied from Sangon Biotechnology Co., Ltd. (Shanghai, China) and the sequences of those are shown in Table S1. All the reagents were analytical grade and used without further purification. Ultrapure water (18.2 MΩ cm) was used throughout the whole experiments, and obtained from a Millipore system (Millipore Corp., Bedford, MA).

Table S1. The DNA sequences used in this work.

Name	Sequence (5′→3′)
Substrate strand DNA1	5’-ACTCACTATrAGGAAGAGATG-$(CH_2)_6$-SH-3’
Catalytic strand DNA2	5’-NH_2-$(CH_2)_6$-CATCTCTTCTCCGAGCCGGTCGAAATAGTGAGT-3’

[a] rA represents adenosine ribonucleotide.

The UV-vis absorption spectra were taken with a UV-2500 UV-vis spectrophotometer (LabTech, China). The morphologies and structures of the prepared materials were characterized by transmission electron microscopy (TEM) (Tecnai G2 F20 S-TWIN, Holland), scanning electron microscopy (SEM) (JSM-6700F, Japan) and powder X-ray diffraction (PXRD, D/MAX-RA, Japan). The chemical composition of TiO_2/Au hybrids and the chemical states of the related elements were investigated by X-ray photoelectron spectroscopy (XPS, ESCALAB250Xi). Fourier transform infrared (FTIR) spectrum was obtained at a Fourier transform spectrometer (NICOLET6700). A PLS-SXE 300 Xe lamp was used as the light source in the PEC test (wavelength, 320-2500 nm; light intensity, 36 mW cm^{-2}). The electrochemical and photoelectrochemical measurements were performed on an electrochemical workstation (CHI 660D, Chenhua Instrumental Co., Shanghai, China) with a typical three-electrode configuration at ambient temperature. The modified ITO slice was served as the working electrode. A Pt wire was used as

auxiliary electrode , and reference electrode was a saturated calomel electrode (SCE). 0.1 M phosphate buffer solution (PBS, pH 7.4) containing 0.1 M AA was utilized as the PEC electrolyte solution.

2. Synthesis of Au NPs decorated TiO_2 hybrids

The Au NPs decorated TiO_2 (TiO_2/Au hybrids) was prepared as the reported work with appropriate modification.[1] Firstly, TiO_2 powders (250 mg) were added in the $HAuCl_4$ solution (0.01 wt.%, 25 mL) in 50 mL flask and the solution was treated ultrasonically to disperse TiO_2 powders. Subsequently, $NaBH_4$ solution (20 mM, 1.5 mL) was added into the solution to perform reduction reaction at room temperature. The reduction procedure for the preparation of Au NPs was different from that reported in the literature.[1] Finally, the resultant solution was centrifuged, and washed by ultrapure water. For future use, 1 mg mL^{-1} TiO_2/Au suspension was prepared and stored in the dark at 4 °C.

3. Preparation of CdS QDs labeled DNA2

The mercaptopropionic acid (MPA)-capped CdS QDs were obtained as the reported work with slight modification.[2] After $CdCl_2{\cdot}2.5H_2O$ was dispersed in ultrapure water (40 mL) and the solution (20 mM Cd^{2+}) was stirred at 80 °C with nitrogen bubbling, MPA (172 μL) was added. Under nitrogen atmosphere, the pH value of the mixture was adjusted to 11 by 1 M NaOH solution. Subsequently, thioacetamide (TAA) solution (0.2 M, 4 mL) was added into the above solution to obtain MPA-capped CdS

QDs. The volume and concentration of TAA used in this work were different from that reported in the literature.[2] After 2 h at 80 °C, a bright yellow MPA-capped CdS QDs solution was obtained, and kept at 4 °C for future use.

According to the preparation process reported in the literature,[3] the MPA-capped CdS QDs and the aminated-DNA2 were conjugated by amide bond. The details are as follows: 10 mg EDC and 10 mg NHS were added into 1.0 mL of 2.0 mg mL^{-1} MPA-capped CdS QDs. The solution was gently shaken for 0.5 h at room temperature. After centrifugation and re-dispersion in 1 mL 40 mM Tris-acetate (pH 8.0), 200 μL of 0.2 μM DNA2 was added, and then the mixture was gently shaken for 12 h at 4 °C, followed by centrifuging and washing with 40 mM Tris-acetate (pH 8.0). Finally, the obtained MPA-capped CdS QDs-labeled DNA2 (DNA2-CdS QDs) was re-dispersed into 1 mL 40 mM Tris-acetate (1mM EDTA, pH 8.0) and kept at 4 °C. The role of EDTA in the buffer solution is to protect the integrity of DNA2.

4. Fabrication of the developed PEC biosensor and Pb^{2+} assay

Before modification, the ITO electrodes were cleaned with acetone, 1 M NaOH in ethanol/water mixture (v/v, 1:1) and H_2O, and dried at 60 °C, as reported in the literatures.[4,5] The role of NaOH is to remove the organic pollutants from the ITO surface. Initially, 20 μL of 1 mg mL^{-1} TiO_2/Au suspension was coated onto the ITO electrode. The TiO_2/Au hybrids modified electrode was dried naturally in air. Following that, the ITO/TiO_2/Au electrode was calcined at 450 °C for 30 min and then cooled to room temperature. Then, 20 μL of 1 μM DNA1 (note: prior to use, the

thiolated oligonucleotide was dissolved in 40 mM Tris-acetate (pH 8.0) containing 10 mM TCEP and 1mM EDTA to break any disulfide bonds between DNA molecules) was dripped on the ITO/TiO_2/Au electrode for 16 h at 4 °C to immobilize DNA1 on the electrode surface via the interaction of thiol groups of DNA1 with the decorated Au NPs on TiO_2, following by washing with 50 mM Tris-acetate (pH 7.5) three times. Subsequently, 20 μL of 2 mM MCH was coated on the electrode at room temperature to passivate possible active sites. After rinsed with 50 mM Tris-acetate (pH 7.5) three times, the electrode was incubated with 20 μL of the prepared DNA2-CdS QDs for 2 h at 37 °C, following by washing with 50 mM Tris-acetate (pH 7.5) three times. Eventually, the above electrode was incubated with Pb^{2+} solutions at different concentrations for 1.5 h at 37 °C. After the electrode was carefully rinsed with 50 mM Tris-acetate (pH 7.5), the PEC detection was carried out in 0.1 M PBS (pH 7.4) containing 0.1 M AA at -0.1 V.

5. XPS survey spectrum of TiO_2/Au hybrids

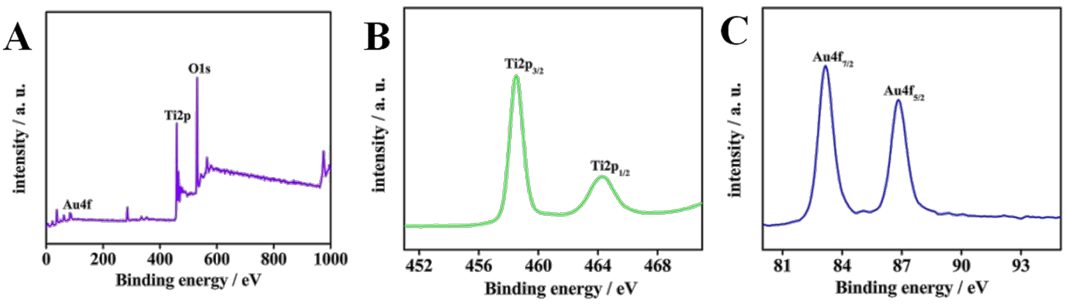

D

Element	Ti	O	Au
XPS Atom %	31.99	67.29	0.72

Fig. S1. (A) XPS survey spectrum of TiO_2/Au hybrids. Related high-resolution

spectra of (B) Ti 2p and (C) Au 4f. (D) Atom% calculated from XPS results of TiO_2/Au hybrids.

According to the XPS results of TiO_2/Au hybrids, the mass ratio of TiO_2/Au is calculated to be 18:1.

6. Characterization of MPA-capped CdS QDs and DNA2-CdS QDs

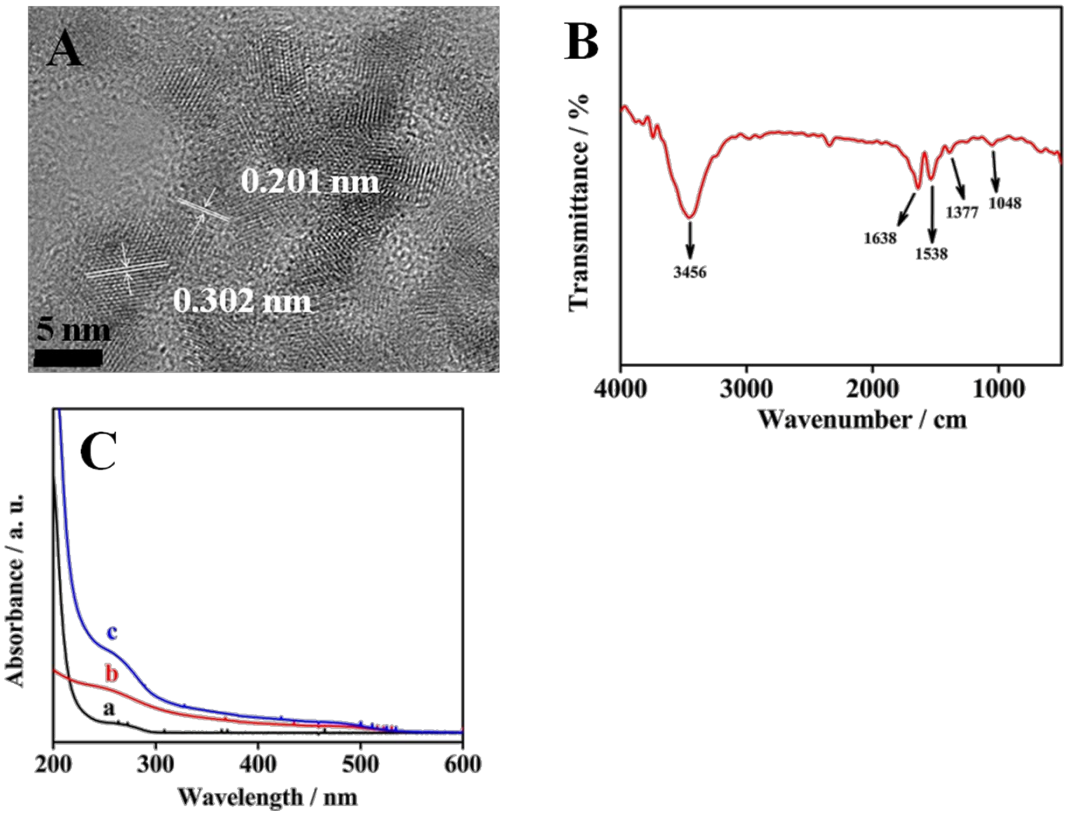

Fig. S2. (A) HRTEM image and (B) FTIR spectrum of MPA-capped CdS QDs (C) UV-vis absorption spectra of DAN2 (a), MPA-capped CdS QDs (b) and DNA2-CdS QDs (c).

The MPA-capped CdS QDs were investigated by high resolution transmission electron microscopy (HRTEM) and FTIR spectroscopy, respectively. As shown in Fig. S2A, the as-prepared MPA-capped CdS QDs have an average diameter of about 5 nm

and the lattice parameters of 0.201 nm and 0.302 nm corresponding to (220) and (111) planes of CdS QDs. Fig. S2B shows the FTIR spectrum of MPA-capped CdS QDs. The broad band centered at 3456 cm^{-1} and absorption peak at 1638 cm^{-1} should be attributed to the surface-adsorbed water molecules.[6] The characteristic absorption bands at 1377 and 1048 cm^{-1} are from the vibrations of Cd-S bond.[7] The peak at 1538 cm^{-1} corresponds to the stretching vibration of COO^-,[8] indicating the presence of carboxyl groups. These results indicate that the successful preparation of MPA-capped CdS QDs.

On the other hand, the UV-vis absorption spectra are shown in Fig. S2C. The DNA2 displays an inherent characteristic absorption peak at 260 nm (curve a). Compared with MPA-capped CdS QDs which exhibit broad light absorption from 550 nm to low wavelengths (curve b), the characteristic absorption of DNA2 is observed for DNA2-CdS QDs (curve c), revealing the successful preparation of DNA2-CdS QDs.

7. Possible mechanism of photocurrent generation

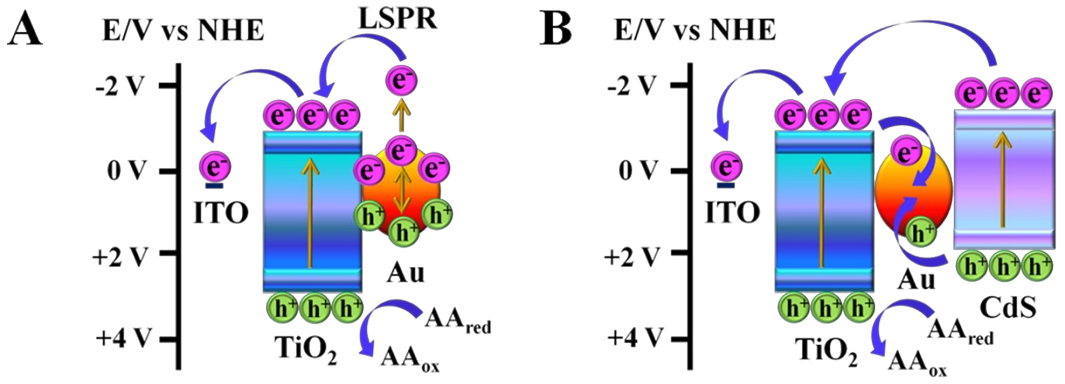

Fig. S3. (A) Migration of LSPR-induced hot electrons of Au NPs to CB of TiO_2. (B)

Possible charge transfer mechanism in the "Z-Scheme" TiO_2/Au/CdS system.

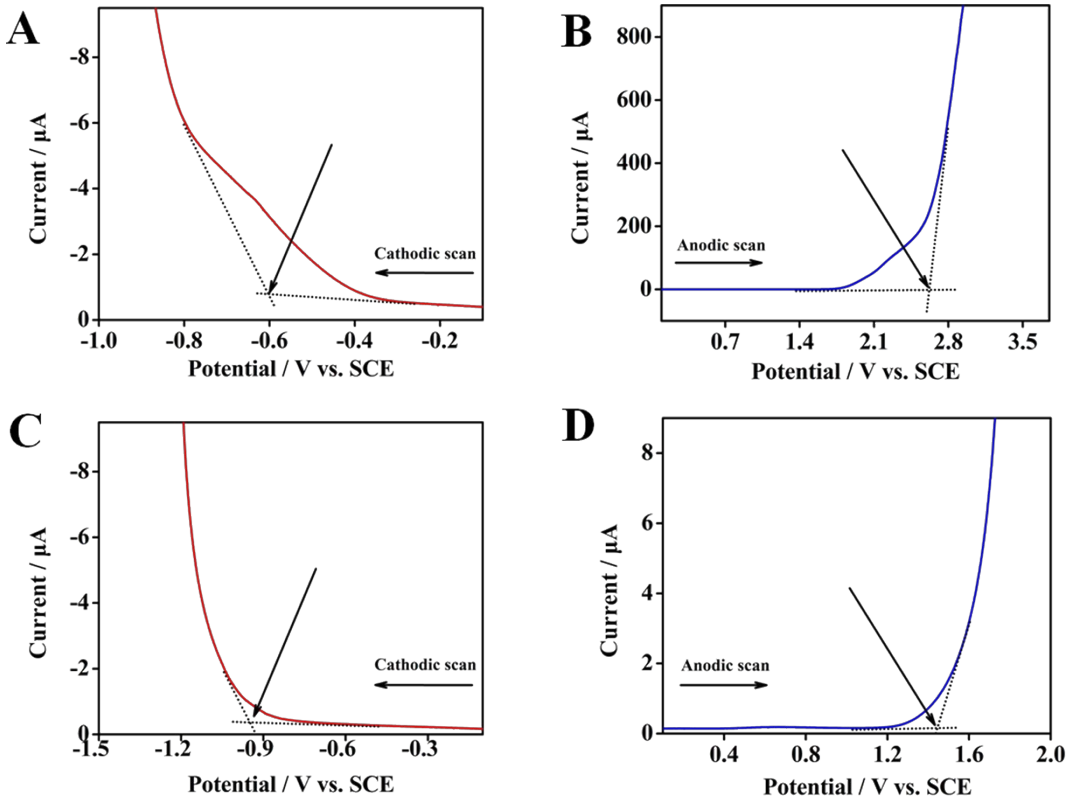

Fig. S4. Cathodic and anodic linear potential scans for determining the conduction band (CB) and valence band (VB) edges of TiO_2 (A, B) and MPA-capped CdS QDs (C, D) in N_2-saturated 0.1 M PBS (pH 7.4).

For the TiO_2/Au (Fig. S3A), TiO_2 and Au NPs can be excited under incident light irradiation. The LSPR effect results in the generation of electron-hole pairs within the Au NPs, and the hot electrons of Au NPs can be injected to the CB of TiO_2, followed by transferring to ITO electrode.[9-11] In this situation, the Au NPs serve as the plasmonic photosensitizer, thus amplifying photocurrent signal.

In order to obtain the possible charge transfer mechanism in the TiO_2/Au/CdS system, the conduction band (CB) and valence band (VB) edges of TiO_2 and MPA-

capped CdS QDs were investigated by electrochemical method,[12,13] and the results are shown in Fig. S4. The values of the CB and VB edges of TiO_2 (MPA-capped CdS QDs) are -0.60 (-0.95) and 2.60 (1.45) V *vs.* saturated calomel electrode (SCE), respectively. That is, the CB and VB potentials of TiO_2 (MPA-capped CdS QDs) are -0.36 (-0.71) and 2.86 (1.69) V *vs.* the normal hydrogen electrode (NHE), respectively. These values are roughly consistent with that reported in the literatures.[14,15]

According to results from Fig. S4, the possible charge transfer mechanism in the "Z-Scheme" TiO_2/Au/CdS system is presented in Fig.S3B. With the illumination of incident light, TiO_2 and MPA-capped CdS QDs are excited to generate photogenerated electron-hole pairs, respectively. The photogenerated electrons in the CB of TiO_2 migrate to Au NPs, and simultaneously, the photogenerated holes in the VB of MPA-capped CdS QDs move to Au NPs to recombine with the photogenerated electrons of TiO_2.[16,17] This charge transfer has a tremendously large driving force, owing to the CB potential of TiO_2 is much negative than the VB potential of MPA-capped CdS QDs (Fig. S4). The matched energy levels of TiO_2 and MPA-capped CdS QDs confirm the successful formation of the "Z-scheme" TiO_2/Au/CdS QDs system. In this system, Au NPs act as "Z-scheme" bridge, which is advantageous in the separation and transportation of photogenerated charges. The accumulated photogenerated electrons at the CB of MPA-capped CdS QDs transfer to the CB of TiO_2 and then transfer to ITO electrode, generating an anodic photocurrent.[17] Meanwhile, photogenerated holes in VB of TiO_2 can be effectively captured by AA to reduce the recombination of photogenerated electron-hole pairs. Therefore, an

enhanced photocurrent signal is obtained.

8. Optimization of experimental conditions

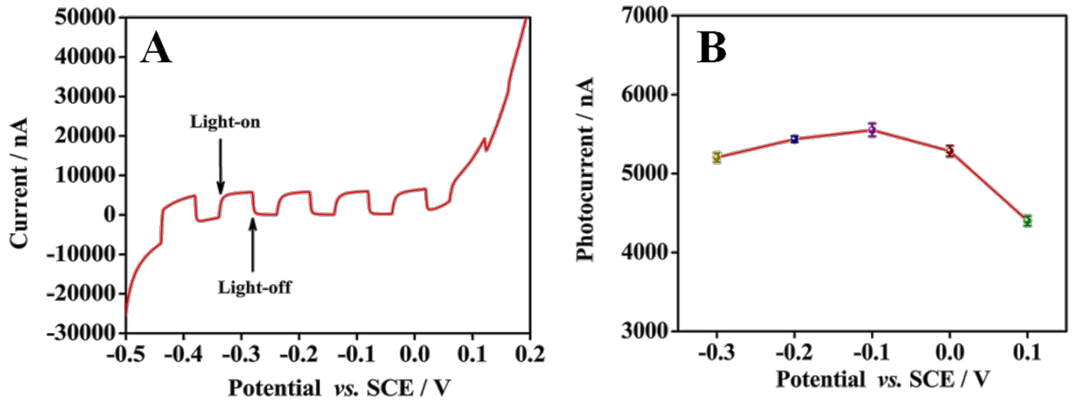

Fig. S5. (A) LSV results of the PEC biosensor under chopped illumination. (B) The effect of applied potential on photocurrents of the PEC biosensor. All the measurements were carried out in 0.1 M PBS (pH 7.4) containing 0.1 M AA.

The developed PEC biosensor was investigated by linear sweep voltammetry (LSV) under chopped illumination. As shown in Fig. S5A, the current values don't significantly change from -0.3 to 0 V. With the increase of applied potential from 0.1 V, the light-off current increases obviously, which may result in the instability of the modified electrode. On the other hand, the large negative potential (< -0.4 V) can lead to the serious reduction reaction. Therefore, the applied potential was further optimized from -0.3 to 0.1 V, and the related results are shown in Fig. S5B. It is noted that the photocurrent signal slightly decreases when the applied potential is from -0.1 to -0.3V, which is attributed to that the negative applied potential inhibits the transfer of the photogenerated electrons from the photoelectric materials to electrode.[18] And, photocurrent signal decreases with the increase of applied potential from -0.1 to 0.1V, probably owing to the oxidation of the photoelectric materials. Hence, -0.1 V is

chosen as the optimal applied potential for PEC assay.

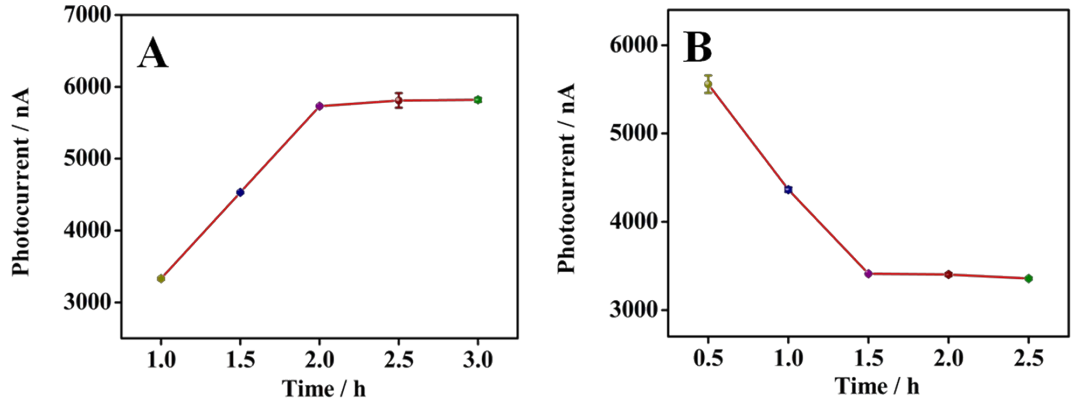

Fig. S6. The effects of (A) hybridization time between DNA1 and DNA2-CdS QDs and (B) incubation time of Pb^{2+} on photocurrents of the developed PEC biosensor.

The hybridization time between DNA1 and DNA2-CdS QDs and the incubation time of Pb^{2+} can affect the analytical performance for the PEC biosensor. Hence, these parameters were optimized.

As shown in Fig. S6A, the photocurrent signal increases with the increase of the hybridization time between DNA1 and DNA2-CdS QDs, due to that more MPA-capped CdS QDs are introduced on the electrode surface. Then, the photocurrent signal reaches a plateau at 2 h, owing to the saturation of hybridization reaction. Thus, 2 h is chosen as the optimal hybridization time.

As another crucial factor, the incubation time of Pb^{2+} was also investigated. From Fig. S6B, the photocurrent signal decreases with the increase of the incubation time, because the more DNA1 strands are cleaved by Pb^{2+}-specific DNAzymes and the more DNA2-CdS QDs are released from the electrode surface. Subsequently, the photocurrent signal reaches a plateau at 1.5 h. This implies that 1.5 h is enough for the above processes. Thus, 1.5 h is utilized as the optimal incubation time of Pb^{2+}.

9. Comparison of different methods for Pb^{2+} assay

Table S2. Comparison of different methods for Pb^{2+} assay.

Method	Linear response range	Detection limit	S (nA pM^{-1})[a]	Reference
Colorimetry	1-15 nM	59.39 nM	-	19
Electrochemistry	0.005-1000 nM	2 pM	-	20
Electrochemistry	0.1 nM-5 μM	45.8 pM	-	21
Electrochemistry	5 pM-1 μM	1.67 pM	-	22
Fluorescence	100 pM-10 μM	50 pM	-	23
Fluorescence	0.001 nM-10 nM	1 pM	-	24
Photoelectrochemical	500 pM-900 nM	166 pM	6.7×10^{-5}	25
Photoelectrochemical	1-500 nM	0.3 nM	0.1	26
Photoelectrochemical	0.1-50 nM	0.05 nM	17.2	27
Photoelectrochemical	0.5 pM-10 nM	0.13 pM	250	This work

[a]S (Sensitivity) = $|I_0-I|/C$, where I_0 is photocurrent of the biosensor incubated without Pb^{2+}, and I is photocurrent of the biosensor incubated with Pb^{2+} at the lowest

concentration (*C*) within the linear response range.

10. The recovery test of Pb^{2+} in tap water and diluted human serum samples

Table S3. The recovery test of Pb^{2+} in tap water and diluted human serum samples.

Sample	Added (pM)	Found* (pM)	Recovery (%)	RSD (%)
Tap water	10	10.13	101.3	0.70
	100	99.70	99.7	3.74
	1000	1001.62	100.2	8.84
Serum samples	10	9.73	97.3	1.83
	100	99.82	99.8	3.07
	1000	1006.64	100.7	0.69

*Average value of three measurements.

To investigate the practical applicability of the developed biosensor for Pb^{2+} assay in real samples, the recovery tests were performed by adding Pb^{2+} into the tap water and diluted human serum samples. The average recoveries for the added Pb^{2+} with 10 pM, 100 pM and 1000 pM are found to be 101.3%, 99.7%, 100.2% in tap water and 97.3%, 99.8%, 100.7% in diluted human serum samples, respectively (Table S3). These indicate that the developed PEC biosensing platform possesses good applicability for Pb^{2+} assay in water and human serum samples, demonstrating great potential for practical applications in environment monitoring and clinical analysis.

11. References

1 X. X. Yan, J. J. Li, R. Y. Yang, Y. M. Li, X. H. Zhang, J. H. Chen, *Sens. Actuators, B.*, 2018, **255,** 2187−2193.

2 M. Zhao, G.-C. Fan, J.-J. Chen, J.-J. Shi, J.-J. Zhu, *Anal. Chem.,* 2015, **87,** 12340−12347.

3 Y. H. He, Z. F. Fan, *Sens. Actuators, B.,* 2018, **257,** 538−544.

4 Z. Y. Yan, Z. H. Wang, Z. Miao, Y. Liu, *Anal. Chem.* 2016, **88,** 922–929.

5 M. Zhao, G.-C.Fan, J.-J. Chen, J.-J. Shi, J.-J. Zhu, *Anal. Chem.* 2015, **87,** 12340–12347.

6 G. D. Yang, Z. Jiang, H. H. Shi, T.C. Xiao, Z. F. Yan, *J. Mater. Chem.,* 2010, **20,** 5301–5309 .

7 F. Jiang, T. T. Yan, H. Chen, A. W. Sun, C. M. Xu, X. Wang, *Appl. Surf. Sci.,* 2014, **295,** 164–172.

8 C. Yi, Y. M. Sun, B. Song, W. W. Tian, Q. Qi, Y. P. Zheng, Y. Q. Dai, W. Jiang, *Nanotechnology,* 2013, **24,** 435704.

9 J. Shu, Z. L. Qiu, S. Z. Lv, K. Y. Zhang, D. P. Tang, *Anal. Chem.,* 2018, **90,** 2425−2429.

10 H. Li, F. Qin, Z. P. Yang, X. M. Cui, J. F. Wang, L. Z. Zhang, *J. Am. Chem. Soc.,* 2017, **139,** 3513−3521.

11 R. Y. Li, R. Yan, J. C. Bao, W. W. Tu, Z. H. Dai, *Chem. Commun.,* 2016, **52,** 11799−11802.

12 G.-L. Wang, J.-X. Shu, Y.-M.Dong, X.-M. Wu, W.-W.Zhao, J.-J. Xu, H.-Y. Chen, *Anal. Chem.,* 2015, **87,** 2892−2900.

13 L.-Y. Jin, Y.-M. Dong, X.-M. Wu, G.-X. Cao, G.-L. Wang, *Anal. Chem.,* 2015, **87,** 10429−10436.

14 T. Wang, Y. Y. Chai, D. K. Ma, W. Chen, W. W. Zheng, S. M. Huang, *Nano Res.,* 2017, **10,** 2699−2711.

15 L. N. Kong, X. T. Zhang, C. H. Wang, J. P. Xu, X. W. Du, L. Li, *Appl. Surf. Sci.,* 2018, **448,** 288−296.

16 H. Tada, T. Mitsui, T. Kiyonaga, T. Akita, K. Tanaka, *Nat. Mater.,* 2006, **5,** 782−786.

17 Q. C. Ma, X. N. Peng, M. L. Zhu, X. N. Wang, Y. Y. Wang, H. Wang, *Electrochem. Commun.,* 2018, **95,** 28−32.

18 H. Dai, Y. L. Li, S. P. Zhang, L. S. Gong, X. H. Li, Y. Y. Lin, *Sens. Actuators, B.,* 2016, **222,** 120−126.

19 Z. J. Huang, J. M. Chen, Z. W. Luo, X. Q. Wang, Y. X. Duan, *Anal. Chem.,* 2019, **91,** 4806−4813.

20 Y. J. Yu, C. Yu, Y. Z. Niu, J. J. Chen, Y. L. Zhao, Y. C. Zhang, R. F. Gao, J. L. He, *Biosens. Bioelectron.,* 2018, **101,** 297−303.

21 R.-N. Ma, L.-L. Wang, M. Zhang, L.-P. Jia, W. Zhang, L. Shang, W.-L. Jia, H.-S. Wang, *Sens. Actuators, B.,* 2018, **257,** 678−684.

22 Y. G. Wang, G. H. Zhao, Q. Zhang, H. Wang, Y. Zhang, W. Cao, N. Zhang, B. Du, Q. Wei, *Sens. Actuators, B.,* 2019, **288,** 325−331.

23 J. F. Pan, Q. Li, D. H. Zhou, J. Chen, *New J. Chem.,* 2019, **43,** 5857−5862.

24 J. Wang, Z. Y. Zhang, X. Gao, X. D. Lin, Y. Q. Liu, S. Wang, *Sens. Actuators, B.,* 2019, **282,** 712−718.

25 H.-M. Deng, L.-J. Huang, Y.-Q. Chai, R. Yuan, Y.-L. Yuan, *Anal. Chem.,* 2019, **91,** 2861−2868.

26 L. J. Huang, H. M. Deng, X. Zhong, M. H. Zhu, Y. Q. Chai, R. Yuan, Y. L. Yuan, *Biosens. Bioelectron.,* 2019, **145,** 111702.

27 Y. Zang, J. P. Lei, Q. Hao, H. X. Ju, *ACS Appl. Mater. Interfaces.,* 2014, **6,** 15991−15997.